Journal of Magnetism and Magnetic Materials 393 (2015) 498–501

Contents lists available at ScienceDirect

Journal of Magnetism and Magnetic Materials

journal homepage: www.elsevier.com/locate/jmmm

Monte-Carlo modeling of exchange bias properties in amorphous magnets

Yong Hu, An Du *

College of Sciences, Northeastern University, Shenyang 110819, China

ARTICLE INFO

Article history:
Received 21 September 2014
Received in revised form
6 February 2015
Accepted 12 June 2015
Available online 18 June 2015

Keywords:
Amorphous magnet
Exchange bias
Magnetization reversal
Monte Carlo simulation

ABSTRACT

We explore the effect of interfacial disorder on exchange bias properties of a soft ferromagnet with a negligible intrinsic anisotropy exchange coupled to a hard amorphous magnet with a random magnetic anisotropy, based on an extensive Monte Carlo simulation. The interfacial disorder is introduced by using a '$\pm J$" model. As compared to the conventionally crystalline ferromagnet/antiferromagnet bilayers, pronounced values and sign inversion in the exchange field are obtained at low temperature after cooling even under a weak field. However, the coercivity in the amorphous system not only shows smaller values, but also exhibits an opposite trend. Different from the ordered crystalline systems, the intrinsic properties of the Harris–Plischke–Zuckermann Hamiltonian rather than the domain structure determine the coercive fields and the shapes of hysteresis loops with different temperatures and cooling fields in the random magnetic anisotropy model, and hence the exchange bias. This theoretical work opens a new avenue for magnetism of the exchange bias and for its applications.

1. Introduction

Giant magnetoresistance (GMR) devices are widely used in read heads of ultrahigh density magnetic recording systems and magnetic sensors [1]. Generally, they comprise a magnetic reference layer and a free magnetic layer, and the direction of magnetization in the reference layer is required to keep constant within the field range being measured ideally. This can be achieved by attaching an antiferromagnet (AFM) to generate an exchange bias (EB) effect [2]. The EB coupling, characterized by a hysteresis loop shifted away from the origin by the amount termed the exchange field (H_E), is very complex, and many questions on the microscopic mechanism of the phenomenon are still open [3]. On the other hand, some recent studies have supported the argument that EB is not necessarily due to the presence of an AFM phase [4–7]. For instance, high values of H_E have been induced in amorphous rare-earth-transition metals (RE-TM) experimentally [8,9]. However, what has happened to the amorphous magnet (AM) and what is the nature of the amorphous interface are still controversial issues.

In this paper, an extremely soft ferromagnet (FM) without any intrinsic anisotropy is used as a pinned layer, while the pinning layer is either an AM with a random magnetic anisotropy (RMA) or an AFM for comparison. Meanwhile, we assume that competing FM/AFM interfacial couplings exist at the FM/AM or FM/AFM interface, and their proportion is allowed to vary to study their special role in establishing EB.

2. Model and Monte Carlo simulation

Four FM monolayers are considered to be exchange coupled to an AM or AFM layer with the same thickness, forming a bilayer structure. Its lateral size is 100×100 and in the film plane the periodic boundary conditions are used to eliminate the finite-size effect. At the atomic level, the planar system can be represented by a simple cubic lattice. In the presence of an external magnetic field (H), the Hamiltonian can be described as

$$H = -J_{FM} \sum_{<i\in FM, j\in FM>} S_i \cdot S_j - H \sum_{i\in FM} S_i - J_A \sum_{<i\in A, j\in A>} S_i \cdot S_j - K_A \sum_{i\in A} (S_i \cdot \hat{e}_i)^2 - H \sum_{i\in A} S_i - J_{IF} \sum_{<i\in FM, j\in A>} S_i \cdot S_j, \quad (1)$$

where S_i denotes the atomic spin at site i and $\hat{e}_i$ denotes the unit vector in the direction of the easy axis at site i. Remarkably, the first line in Eq. (1) gives the energy of the soft FM layer which consists of the nearest-neighbor exchange energy and the Zeeman energy. The FM exchange coupling constant $J_{FM} = 1$, serving as an

* Corresponding author. Fax: +86 24 8367 8686.
E-mail address: duanneu@126.com (A. Du).

http://dx.doi.org/10.1016/j.jmmm.2015.06.025
0304-8853/

energy unit to normalize other parameters, and H is applied perpendicular to the film plane. Therefore, the intrinsic magnetic parameters including exchange (J) and anisotropy (K) constants are in units of J_{FM}, while the extrinsic ones H in units of $J_{FM}/g\mu_B$, temperature (T) in units of J_{FM}/k_B. Next, the energy contribution of the hard AM or AFM layer is listed in the second line of Eq. (1). Besides the nearest-neighbor exchange and Zeeman energies, a uniaxial magnetocrystalline anisotropy energy term is included. If the hard magnet is AM, the RMA model of Harris, Plischke, and Zuckermann (HPZ) is used [10], where its exchange coupling constant is $J_A = J_{AM} = J_{FM}$, anisotropy constant $K_A = K_{AM} = 10J_{FM}$, and $\hat{e}_i$ a random unit vector. Otherwise, for the AFM phase, $J_A = J_{AF} = -J_{FM}$, $K_A = K_{AF} = 10J_{FM}$, and $\hat{e}_i$ perpendicular to the film plane. Finally, the interfacial exchange energy between the FM and AM (or AFM) layers with the absolute value of exchange coupling constant $|J_{IF}| = J_{FM}$ is considered, and in order to highlight the disorder and defect of the frustrated interface, the coexistence of FM and AFM interfacial couplings is postulated [11]. To quantify such a disorder at the interface we define p as the fraction of AFM interfacial coupling and thus the fraction of the FM one is $1 - p$.

The standard Metropolis algorithm with local dynamics is used to calculate the orientation of spins in metastable states responsible for hysteresis [12]. For spin updates in every Monte Carlo step (MCS), the new spin vector direction is adjusted randomly only in a confined range, and the angular deviation amplitudes for polar and azimuthal angles are $\delta\theta = \pi/12$ and $\delta\varphi = \pi/6$, causing a constrained acceptance rate. In the simulation, the bilayers in which the FM spins are aligning perpendicular to the film plane while the AM or AFM ones are randomly oriented are cooled from a temperature $T_0 = 2J_{FM}/k_B$, which is higher than the magnetic transition temperatures of the pinning layers, to a desired T in a constant step of $\delta T = 0.1J_{FM}/k_B$, under a given magnetic field, so-called cooling field (H_{FC}). Then, at the T, the hysteresis loop is recorded by cycling H from $3J_{FM}/g\mu_B$ to $-3.0J_{FM}/g\mu_B$ in a constant step of $\delta H = 0.02J_{FM}/g\mu_B$. At every step of T and H, 5×10^3 MCSs per spin are performed to equilibrate the system, succeeded by a run of 5×10^3 MCSs per spin for averaging the magnetization. The sweep rate is slow enough to guarantee the quasiequilibrium state, and the final magnetization is configurationally averaged over ten independent realizations of the initial spin configurations and sets of the unit vectors of the easy axes in the AM or AFM layer to reduce the statistical errors [13–15].

3. Results and discussion

Fig. 1 shows the results of H_E and coercivity (H_C) of the bilayers with an AM or AFM layer at *low T* after cooling under different H_{FC}. Their quantities are calculated through $H_E = (H_R + H_L)/2$ and $H_C = (H_R - H_L)/2$, where H_L and H_R denote the coercive fields at the decreasing and increasing branches of FM hysteresis loops. As for the FM/AM bilayers, H_E is negative and its value decreases with increasing p when p is smaller than 50%. In addition, H_{FC} has a weak effect on H_E in this p range. With further increasing p from 50% to 100%, the role of H_{FC} on the $H_E \sim p$ behavior becomes significant, that is, under weak $H_{FC}H_E$ may be still negative and its value may turn to increase, while under stronger $H_{FC}H_E$ may change its sign and its value may continue increasing. On the other hand, H_C of the FM/AM bilayers with $p = 50\%$ approximately is slightly higher than those with other p, and the stronger H_{FC} may generate a larger H_C only in the p range from 50% to 100%. As for the FM/AFM bilayers, the stronger H_{FC}, is the larger H_E at $p = 0$. However, with increasing p, H_E exhibits an oscillatory behavior around 0, while H_C forms an obvious and symmetrical valley shape with a larger value in comparison to the FM/AM bilayers.

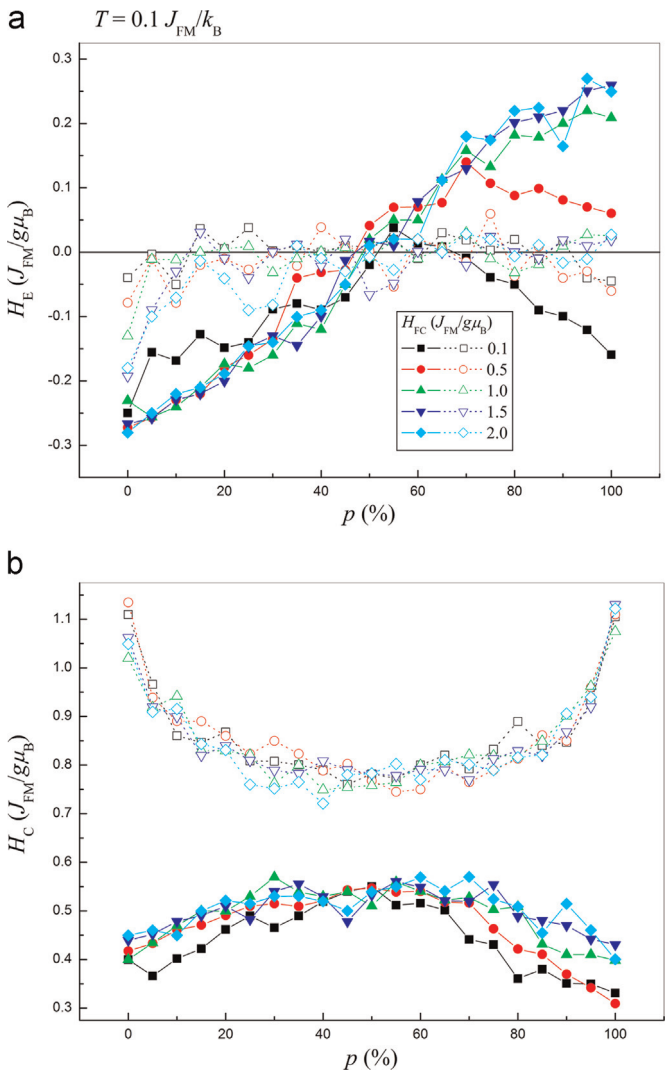

Fig. 1. (a) H_E and (b) H_C as functions of p in the bilayers with an AM (solid symbols and lines) or AFM (open symbols and dotted lines) layer at $T = 0.1J_{FM}/k_B$ after cooling under different fields.

From the H_E results of the FM/AM bilayers, two interesting phenomena are worthwhile to be studied further: (a) pronounced hysteresis loop shift and (b) positive EB. Actually, the positive EB is not new for AFM-based systems [16,17]. However, positive shifts can be observed with large positive H_{FC} while small positive H_{FC} only yield negative shifts as usual, in contradiction to the findings from the FM/AM bilayers in this paper. Furthermore, in the AFM-based systems, the EB effect is related to the uncompensated AFM spins at the interface, which are created during the field-cooling process [18]. It is reminiscent of the weak H_{FC} that is incompetent to induce a pronounced EB at low T since the number of uncompensated spins at the interface is very small, also opposite to the observations in the FM/AM bilayers. In order to interpret the phenomena observed here and demonstrate their origins, the coercive field behaviors versus p in the two kinds of bilayers and the net magnetization in the AM layer (M_{IF}) at different p are presented in Fig. 2, respectively.

In the FM/AM bilayers, similar to the FM/AFM bilayers, a positive M_{IF} exists at low T after field-cooling. However, different from the completely frozen configurations in the FM/AFM bilayers (the results are not shown here), the low-T configurations in the FM/AM bilayers are rearranged constantly especially during the FM magnetization reversal due to the RMA nature in the AM layer.

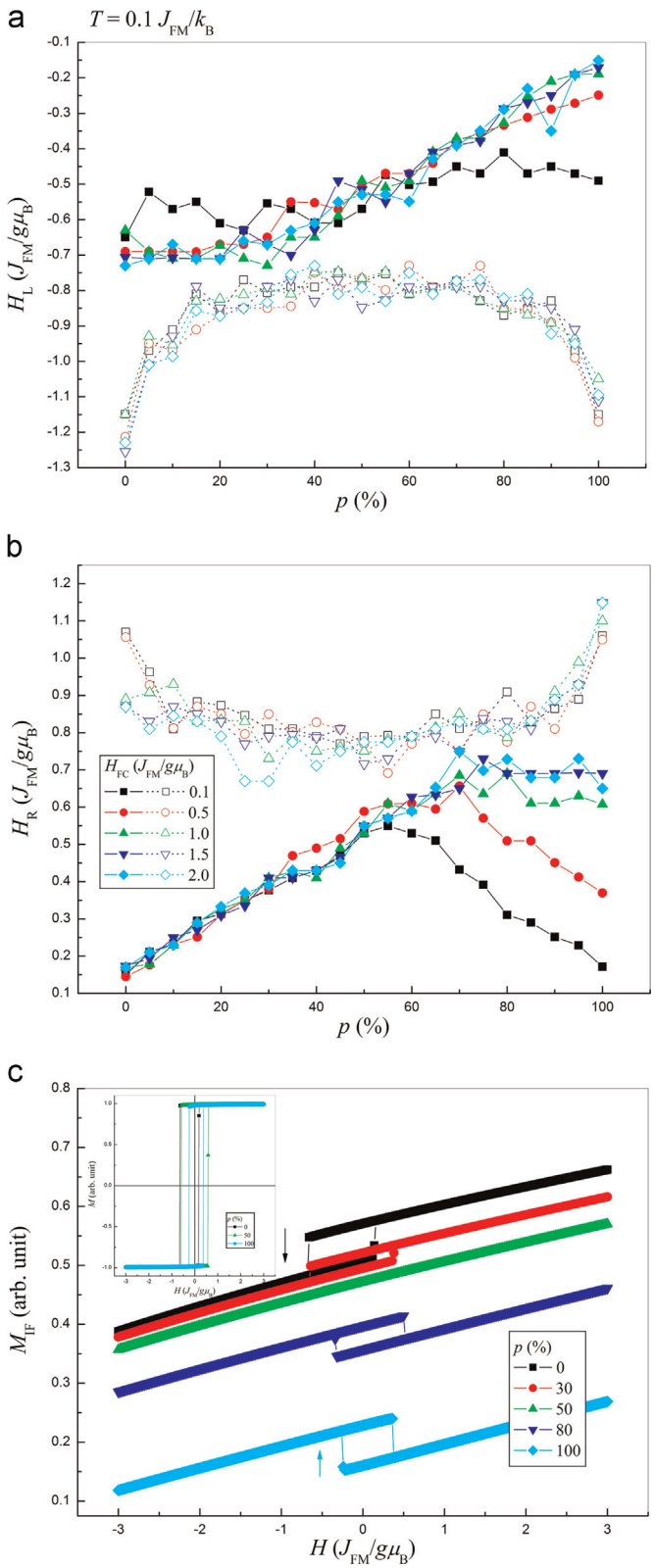

Fig. 2. Coercive fields at the (a) decreasing and (b) increasing branches as functions of p in the bilayers with an AM (solid symbols and lines) or AFM (open symbols and dotted lines) layer at $T = 0.1J_{FM}/k_B$ after cooling under different fields. (c) Net magnetization at the interface in the AM layer as a function of H in the bilayers with representative p at $T = 0.1J_{FM}/k_B$ after cooling under $H_{FC} = 0.5J_{FM}/g\mu_B$, and inset shows the results of FM hysteresis loops.

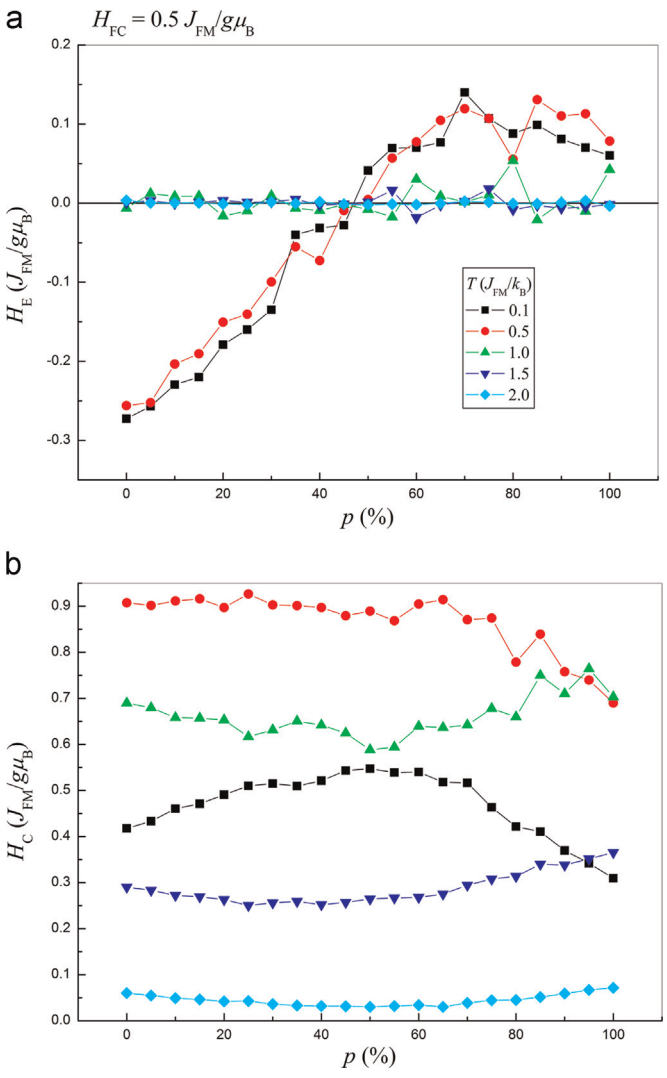

Fig. 3. (a) H_E and (b) H_C as functions of p in the FM/AM bilayers at different T after cooling under $H_{FC} = 0.5J_{FM}/g\mu_B$.

When p is small, the FM coupling at the interface is dominant and some AM spins at the interface change their directions parallel or almost parallel to their nearest neighboring FM spins during the FM magnetization reversal at H_L to lead to a decrease of M_{IF}. On the contrary, with increasing p, the AFM coupling at the interface become more significant and the antiparallel ordering between the nearest neighboring FM and AM spins is more favored, resulting that M_{IF} increases. Remarkably, the FM and their nearest neighboring AM spins reverse towards the same directions at small p, which needs to cost stronger H. Thus H_L increases monotonically with increasing p. At the other side, the positive M_{IF} at the interface encourages the FM magnetization reversal, and for $p < 50\%$, a large M_{IF} induces the FM magnetization reversal at a weak H_R. The $H_R \sim p$ curves are roughly linear and independent of H_{FC}. When $p > 50\%$, H_R becomes to depend on H_{FC} strongly, indicating that the AFM coupling at the interface and H are competing to each other. For a large p, M_{IF} decreases during the FM magnetization reversal at H_R, as discussed above, and the rearrangement of AM spins encourages the FM magnetization reversal simultaneously, resulting in a decrease of H_R again with further increasing p under weak H_{FC}. However, such behaviors are smeared by strong H_{FC} and the decrease of H_R with p is gradually eliminated under strong H_{FC}. Finally, the resultant H_E and H_C are obtained in the FM/AM bilayers and quite different from those in

the FM/AFM bilayers, in which the spin rearrangements in the hard layer are impossible or negligible.

Finally, the dependences of H_E and H_C in the FM/AM bilayers on T are briefly discussed and the results are given in Fig. 3. Interestingly, at the different low T below $T_B \approx 0.75$ where EB vanishes, not only H_E changes little, but also the $H_E \sim p$ behavior remains, different from the common results of a rapid decrease of H_E with T in the FM/AFM bilayers. It is implied there is a better thermal stability of H_E in the FM/AM bilayers, possibly because in the AM layer the RMA induces a wider energy barrier distribution and is more effective to overcome the thermal fluctuations in the low T range. However, at high enough T above T_B, the energy barriers can also be conquered and H_E almost vanishes. As for H_C, similar to that in the FM/AFM bilayers, H_C is nonmonotonic with T and exhibits a peak around T_B. Moreover, H_C becomes independent of p at high T.

4. Conclusion

We perform an extensive Monte Carlo simulation to study the EB properties when the conventional AFM layer is replaced by an AM layer with RMA in the bilayers. At low T after cooling under a weak H_{FC}, a pronounced and/or positive EB effect may be obtained in the FM/AM bilayers, implying that a higher sensitivity exists for the AM phase to H_{FC}, T, etc. Additionally, it is demonstrated that the RMA can be a new source of EB, and through properly adjusting the morphology of interface, the control of EB is possible.

Acknowledgments

The research was sponsored by National Natural Science Foundation of China under Contract no. 11204026, Fundamental Research Funds for the Central Universities under Contract no. N130405010, and Informalization Construction Project of Chinese Academy of Sciences during the 11th Five-Year Plan Period under contract nos. INFO-115-B01 and ZDY2008-2-A12.

References

[1] M.N. Baibich, J.M. Broto, A. Fert, F. Nguyen van Dau, F. Petroff, P. Etienne, G. Creuzet, A. Friederich, J. Chazelas, Phys. Rev. Lett. 61 (1988) 2472.
[2] W.H. Meiklejohn, C.P. Bean, Phys. Rev. 102 (1956) 1413.
[3] J. Nogués, J. Sort, V. Langlais, V. Skumryev, S. Suriñach, J.S. Muñoz, M.D. Baró, Phys. Rep. 422 (2005) 65.
[4] M. Ali, P. Adie, C.H. Marrows, D. Greig, B.J. Hickey, R.L. Stamps, Nat. Mater. 6 (2007) 70.
[5] S. Mangin, G. Marchal, B. Barbara, Phys. Rev. Lett. 82 (1999) 4336.
[6] H.M. Nguyen, P.Y. Hsiao, M.H. Phan, J. Appl. Phys. 107 (2010) 09D706.
[7] H.M. Nguyen, C.H. Lee, P.Y. Hsiao, M.H. Phan, J. Appl. Phys. 110 (2011) 043909.
[8] R. Sbiaa, H. Le Gall, Appl. Phys. Lett. 75 (1999) 256.
[9] N.M. Hong, N.H. Dan, N.X. Phuc, J. Magn. Magn. Mater 242–245 (2002) 847.
[10] R. Harris, M. Plischke, M.J. Zuckermann, Phys. Rev. Lett. 31 (1973) 160.
[11] D. Fiorani, L. Del Bianco, A.M. Testa, K.N. Trohidou, Phys. Rev. B 73 (2006) 092403.
[12] D.A. Dimitrov, G.M. Wysin, Phys. Rev. B 54 (1996) 9237.
[13] Y. Hu, Y. Liu, A. Du, F. Shi, Phys. Lett. A 378 (2014) 1667.
[14] Y. Hu, G. Wu, Y. Liu, A. Du, Phys. Lett. A 376 (2012) 1650.
[15] Y. Hu, G.Z. Wu, Y. Liu, A. Du, J. Magn. Magn. Mater. 324 (2012) 3204.
[16] J. Nogués, D. Lederman, T.J. Moran, I.K. Schuller, Phys. Rev. Lett. 76 (1996) 4624.
[17] Y. Hu, A. Du, Phys. Status Solidi B 248 2011–2932; Y. Hu, A. Du, J. Appl. Phys. 102 2007 p. 113911.
[18] Y. Hu, Y. Liu, A. Du, Phys. Status Solidi B 247 (2010) 972.